Molecular and spin dynamics simulations using modern integration methods

Article *in* American Journal of Physics · July 2005

DOI: 10.1119/1.1900096

3 authors:

Shan-Ho Tsai
University of Georgia
65 PUBLICATIONS **1,562** CITATIONS
SEE PROFILE

Lee Hwee-Kuan
Agency for Science, Technology and Research (A*STAR)
124 PUBLICATIONS **1,265** CITATIONS
SEE PROFILE

D. P. Landau
University of Georgia
528 PUBLICATIONS **23,845** CITATIONS
SEE PROFILE

AAPT PHYSICS EDUCATION | AMERICAN JOURNAL of PHYSICS

Molecular and spin dynamics simulations using modern integration methods

Shan-Ho Tsai, H. K. Lee, and D. P. Landau

Citation: American Journal of Physics **73**, 615 (2005); doi: 10.1119/1.1900096
View online: http://dx.doi.org/10.1119/1.1900096
View Table of Contents: http://scitation.aip.org/content/aapt/journal/ajp/73/7?ver=pdfcov
Published by the American Association of Physics Teachers

Molecular and spin dynamics simulations using modern integration methods

Shan-Ho Tsai
Center for Simulational Physics, University of Georgia, Athens, Georgia 30602 and Enterprise Information Technology Services, University of Georgia, Athens, Georgia 30602

H. K. Lee
Department of Physics, Tokyo Metropolitan University, Hachioji, Tokyo 192-0397, Japan

D. P. Landau
Center for Simulational Physics, University of Georgia, Athens, Georgia 30602

(Received 18 May 2004; accepted 4 March 2005)

Decomposition algorithms have proven useful for molecular dynamics and spin dynamics simulations of many-body systems. These methods are time reversible, symplectic, and the error in the total energy is bounded. In general, these techniques are accurate for much larger time steps than more standard integration methods. We review these decomposition algorithms and illustrate their performance for simulations of a Heisenberg ferromagnet. © *2005 American Association of Physics Teachers.*

[DOI: 10.1119/1.1900096]

I. INTRODUCTION

Computer simulations have revolutionized our ability to understand the behavior of many types of models in statistical mechanics.[1] Stochastic sampling (Monte Carlo) provides information about static properties, but cannot elucidate time-dependent properties.[2–4] In contrast, molecular dynamics[5] and spin dynamics[6] simulations are powerful tools for investigating the evolution of physical quantities and hence enhancing our understanding of the dynamic properties of many-body systems. In these simulations the classical equations of motion governing the dynamical properties of the systems are solved numerically. Typically the time scale of the phenomena of interest is much longer than the time steps that can be used in standard finite time difference methods. A large number of integration steps is required, and large truncation errors occur unless the time step is very small. However, small time steps often lead to forbiddingly long computation time, which limits studies of long time scales.

Progress has been accelerated with the advent of new, symplectic methods.[7–10] These numerical methods are based on the decompositions of exponential operators. The methods are time reversible, symplectic, that is, conserve the phase-space volume exactly, and the error in the total energy of the system is bounded.[11,12] (In some cases the total energy of the system is conserved exactly.[13,14]) The effectiveness and efficiency of these symplectic methods have been illustrated by molecular dynamics simulations of proteins in water[11] and spin dynamics simulations of the magnetic excitations in $RbMnF_3$.[15,16] In the latter case, the improved integration method was used to obtain high-resolution results, which were compared directly and quantitatively with neutron-scattering data, yielding good agreement and shedding light on controversies between theory and experiment.[15]

In general, the dynamic properties of a system are more complex than static (time-independent) ones. For example, although the classical Heisenberg ferromagnet and antiferromagnet belong to the same static universality class, they have very different dynamic behavior. This difference already can be seen from linear spin-wave theory, which predicts different low-temperature dispersion curves for the two models.[17]

Historically, pedagogical treatments of the time dependence of systems have been largely restricted to simple models for which exact solutions can be found.[18] Some advanced topics have been treated theoretically with approximate methods.[19] However, much interesting physical phenomena cannot be studied analytically, and the use of numerical methods can greatly expand the range of accessible physical phenomena that can be studied.

In this paper we briefly describe standard integration methods and then review the decomposition algorithms applied to classical molecular dynamics and spin dynamics simulations. In Sec. II we express the classical equations of motion used in molecular dynamics in the Liouville formulation, and in Sec. III we introduce spin dynamics. We discuss criteria for good integration methods in Sec. IV, and briefly review several standard integration algorithms in Sec. V. In Sec. VI we describe the new decomposition algorithms and some numerical tests. Finally, illustrations of spin dynamics results are shown in Sec. VII and a summary is provided in Sec. VIII.

II. MOLECULAR DYNAMICS

Let us consider a system of N particles with masses m_i described by their positions $\mathbf{r}_i$ and velocities $\mathbf{v}_i$, interacting via a potential $u(r_{ij})$, where $r_{ij}=|\mathbf{r}_{ij}|=|\mathbf{r}_i-\mathbf{r}_j|$. The energy of the system can be written as

$$\mathcal{H}=\sum_{i=1}^{N}\frac{1}{2}m_i v_i^2+\sum_{i,j<i}u(r_{ij}), \tag{1}$$

where the force on particle i due to particle j is given by

$$\mathbf{f}_{ij}=-\nabla_{\mathbf{r}_i}u(r_{ij}). \tag{2}$$

The equations of motion are given by

$$m_i \frac{d^2\mathbf{r}_i}{dt^2} = \sum_{j,j\neq i} \mathbf{f}_{ij} \equiv \mathbf{f}_i \quad (i=1,\ldots,N). \tag{3}$$

The evolution of the system can be studied by integrating the equations of motion to obtain $\mathbf{r}_i(t)$ and $\mathbf{v}_i(t)$, for $i=1,2,\ldots,N$. In a Hamiltonian system,[20] the total energy and phase space volume are constants of the motion, that is, they are conserved quantities, and the trajectories of the particles are time reversible.

A. Liouville formulation

The equations of motion, Eq. (3), in classical mechanics also can be written as[20]

$$\frac{dy(t)}{dt} = [y(t),\mathcal{H}], \tag{4}$$

where $y(t)=\{\mathbf{r}_i(t),\mathbf{v}_i(t)\}$ denotes a configuration of the N particles [that is, $y(t)$ consists of the set of positions and velocities of the N particles at time t], and $[y(t),\mathcal{H}]$ is the Poisson bracket of $y(t)$ and $\mathcal{H}$ given by[20]

$$[y(t),\mathcal{H}] \equiv \sum_i \frac{1}{m_i}\left(\frac{\partial y(t)}{\partial \mathbf{r}_i}\cdot\frac{\partial \mathcal{H}}{\partial \mathbf{v}_i} - \frac{\partial y(t)}{\partial \mathbf{v}_i}\cdot\frac{\partial \mathcal{H}}{\partial \mathbf{r}_i}\right). \tag{5}$$

We evaluate the Poisson bracket in Eq. (4) and obtain

$$\frac{dy(t)}{dt} = \hat{L}y(t), \tag{6}$$

where $\hat{L}$ is the Liouville operator defined as

$$\hat{L} \equiv \sum_{i=1}^{N}\left(\mathbf{v}_i\cdot\frac{\partial}{\partial \mathbf{r}_i} + \frac{\mathbf{f}_i}{m_i}\cdot\frac{\partial}{\partial \mathbf{v}_i}\right). \tag{7}$$

Equation (6) is a set of coupled differential equations. The formal solution for Eq. (6) is

$$y(t+\tau) = e^{\hat{L}\tau}y(t), \tag{8}$$

where τ represents a time step, and $e^{\hat{L}\tau}$ is the evolution operator, which governs how $y(t)$ changes with time. Note that the formal solution is exact for any time step τ, not necessarily infinitesimal. Because the formal solution of the equations of motion plays a major role in the decomposition algorithms described in Sec. VI, we have included a derivation of this solution in Appendix A.

III. SPIN DYNAMICS

For simplicity, we discuss spin dynamics simulations for a specific model, namely the classical isotropic Heisenberg model, described by the Hamiltonian

$$\mathcal{H} = -J\sum_{\langle i,j\rangle} \mathbf{S}_i\cdot\mathbf{S}_j, \tag{9}$$

where $\mathbf{S}_i$ is a dimensionless unit vector (a ''classical spin'') located on lattice site i, and nearest-neighbor pairs of spins are coupled by the interaction parameter J, which can be ferromagnetic ($J>0$) or antiferromagnetic ($J<0$). One of the best physical realizations of this model is $RbMnF_3$, for which the magnetic ions Mn^{+2} have a total spin quantum number $S=\frac{5}{2}$, and are located on the sites of a simple cubic lattice. Nearest-neighbor interactions are antiferromagnetic, with $J_{\text{exp}}=-(0.58\pm0.06)$ meV.[21] Magnetic ordering with antiferromagnetic alignment of spins occurs below the critical temperature[22] $T_c=83$ K.

Magnetic ions with spin $S\gtrsim 2$ can be well approximated by classical spins.[23] Quantitative comparison of simulation results obtained from the classical Hamiltonian in Eq. (9) with experimental data require proper normalization of the classical spins or, equivalently, of the interaction parameter J.[15] In this section we consider simple cubic lattices with periodic boundary conditions.

Heisenberg models have true dynamics governed by the equations of motion[24]

$$\frac{d\mathbf{S}_i}{dt} = -\gamma\mathbf{S}_i\times\mathbf{H}_{\text{eff},i}, \tag{10}$$

where γ is the gyromagnetic factor,[24] and the effective field $\mathbf{H}_{\text{eff},i}$ is defined as

$$H^k_{\text{eff},i} = -J\sum_{j=\text{nn}(i)} S^k_j \quad (k=x,y,z), \tag{11}$$

with the sum performed over all nearest-neighbor (nn) sites of i. In computer simulations, constants often are absorbed into variables to simplify the program and reduce floating point errors. In this case, the constant γ is absorbed into the time variable. Hence, for computational purposes we use

$$\frac{d\mathbf{S}_i}{dt} = -\mathbf{S}_i\times\mathbf{H}_{\text{eff},i}. \tag{12}$$

Because the effective field has units of the interaction parameter J, the time variable used in spin dynamics simulations also is measured in units of J, that is, tJ is a dimensionless variable. If we denote

$$\mathbf{S}_i = \begin{pmatrix} S^x_i \\ S^y_i \\ S^z_i \end{pmatrix}, \tag{13}$$

we can then write the equations of motion as

$$\frac{d\mathbf{S}_i}{dt} = \begin{bmatrix} 0 & -H^z_{\text{eff},i} & H^y_{\text{eff},i} \\ H^z_{\text{eff},i} & 0 & -H^x_{\text{eff},i} \\ -H^y_{\text{eff},i} & H^x_{\text{eff},i} & 0 \end{bmatrix}\mathbf{S}_i \equiv R_i\mathbf{S}_i. \tag{14}$$

We write the equations of motion for all spins in matrix form

$$\frac{d}{dt}\begin{pmatrix} \mathbf{S}_1(t) \\ \vdots \\ \mathbf{S}_N(t) \end{pmatrix} = \begin{pmatrix} R_1 & & 0 \\ & \ddots & \\ 0 & & R_N \end{pmatrix}\begin{pmatrix} \mathbf{S}_1(t) \\ \vdots \\ \mathbf{S}_N(t) \end{pmatrix}, \tag{15}$$

where each of the matrix elements $R_1,\ldots,R_N$ is a 3×3 matrix as defined in Eq. (14).

To write the equations of motion in a more succinct form, we let

$$y(t) = \begin{pmatrix} \mathbf{S}_1(t) \\ \vdots \\ \mathbf{S}_N(t) \end{pmatrix}, \quad \hat{R} = \begin{pmatrix} R_1 & & 0 \\ & \ddots & \\ 0 & & R_N \end{pmatrix}, \tag{16}$$

and then write Eq. (15) as

$$\frac{dy(t)}{dt} = \hat{R}y(t). \tag{17}$$

Equation (17) is a set of coupled differential equations, and we have to use numerical methods to integrate them and determine $y(t)$. Note that the spin positions are fixed and the spin motion refers only to the change of spin orientations. The formal solution of Eq. (17) is similar to the Liouville formulation of molecular dynamics,

$$y(t+\tau)=e^{\hat{R}\tau}y(t), \tag{18}$$

where $e^{\hat{R}\tau}$ is the evolution operator. Note that Eqs. (8) and (18) are mathematically equivalent, differing only by the operators $\hat{L}$ and $\hat{R}$. $\hat{L}$ governs the motion of particles in the phase space $\{\mathbf{r}_i,\mathbf{v}_i\}$, and $\hat{R}$ governs the orientational change of the spins in the phase space $\{\mathbf{S}_i\}$.

To obtain the dynamic properties of the spin model at fixed temperature T rather than at fixed energy, we use many equilibrium configurations obtained from Monte Carlo simulations[2] of the model at a given T as initial configurations. Solutions for different initial configurations are then averaged to yield results in the canonical ensemble.

IV. CRITERIA FOR A GOOD INTEGRATION ALGORITHM

Given limited computer resources and the interest in the long time behavior of the equations of motion, the overall speed of the integration algorithm is very important. Each integration step involves force or spin derivative computations, which are very time consuming. To reduce the cpu time for the total integration, it is desirable that an algorithm be accurate for large time steps to reduce the total number of force or spin derivative calculations. The speed of a single integration step is not an important factor to consider.

Another criterion for a good integration method is that it is consistent with the conservation laws and properties of the classical equations of motion. Of particular importance is that it conserve the energy and the phase-space volume, and that it be time reversible. These properties are closely related to the stability of the algorithm and to its accuracy for large time steps.

V. STANDARD INTEGRATION METHODS

Ordinary differential equations often are solved numerically using finite difference methods.[25] The procedure is to use the variables (positions in molecular dynamics, spins in spin dynamics, and their time derivatives) at time t to compute the values of these quantities at a later time $t+\tau$. The accuracy of this procedure often is proportional to a power of τ. An integration method is referred to as an nth-order algorithm if the local (per time step) error in the integrated quantity is $\mathcal{O}(\tau^{n+1})$. Here we briefly review some of the commonly used finite difference methods. To simplify the notation, we will omit the particle label in the variables.

A. Truncated Taylor expansion

The simplest integration method is to write Taylor series expansions such as

$$r(t+\tau)=r(t)+v(t)\tau+\frac{f(t)}{2m}\tau^2+\cdots, \tag{19}$$

and truncate the expansion to $\mathcal{O}(\tau^3)$ for example. Truncation at higher orders of τ requires the computation of higher-order derivatives of positions or spins. Although such computations are possible, usually the resulting method is too complex to be useful. This algorithm is not time reversible [replacing τ by $-\tau$ in Eqs. (19) yields different trajectories], does not conserve the phase-space volume, and gives rise to very large energy drift.

A better implementation of a Taylor series expansion that avoids large energy drift is the popular Verlet algorithm. For brevity we will discuss this algorithm in the next two sections for molecular dynamics only.

B. Position-Verlet algorithm

The Taylor series expansions for the positions at times $t+\tau$ and $t-\tau$, about t, can be written as

$$r(t+\tau)=r(t)+v(t)\tau+\frac{1}{2}\frac{f(t)}{m}\tau^2+\frac{1}{3!}\frac{d^3r}{dt^3}\tau^3+\mathcal{O}(\tau^4), \tag{20}$$

$$r(t-\tau)=r(t)-v(t)\tau+\frac{1}{2}\frac{f(t)}{m}\tau^2-\frac{1}{3!}\frac{d^3r}{dt^3}\tau^3+\mathcal{O}(\tau^4). \tag{21}$$

If we add Eqs. (20) and (21), we have

$$r(t+\tau)=2r(t)-r(t-\tau)+\frac{f(t)}{m}\tau^2+\mathcal{O}(\tau^4). \tag{22}$$

The position-Verlet algorithm consists of using Eq. (22) to determine the evolution of $r(t)$. The first integration step can be done using a truncated Taylor series expansion given by Eq. (19). Note that the computation of the positions at a later time does not explicitly use any velocities, but the velocities are needed for computing the kinetic energy and thus the total energy of the system.

If we subtract Eq. (21) from Eq. (20), we have

$$r(t+\tau)-r(t-\tau)=2v(t)\tau+\mathcal{O}(\tau^3), \tag{23}$$

and the time evolution of velocities can be determined by

$$v(t)=\frac{r(t+\tau)-r(t-\tau)}{2\tau}+\mathcal{O}(\tau^2). \tag{24}$$

The Verlet algorithm is a second-order method that has been widely used in molecular dynamics simulations.[5] It is time reversible [because τ and $-\tau$ enter symmetrically in Eq. (22)], preserves phase-space volume, and although the total energy is not conserved, the long-term energy drift is not very large if a small time step is used. Because it is a second-order method, it is not very accurate for large time steps.

C. Velocity-Verlet algorithm

Another implementation of the Verlet algorithm, known as the velocity-Verlet algorithm, computes the time evolution of the position and velocity by

$$r(t+\tau)=r(t)+v(t)\tau+\frac{1}{2}\frac{f(t)}{m}\tau^2, \tag{25}$$

$$v(t+\tau)=v(t)+\frac{1}{2}\frac{f(t+\tau)+f(t)}{m}\tau. \tag{26}$$

This algorithm corresponds to first computing $r(t+\tau)$ using Eq. (25), then using the new positions to determine the

forces $f(t+\tau)$. Finally, the velocities $v(t+\tau)$ are computed from Eq. (26).

To show the equivalence between the position- and the velocity-Verlet algorithms, we write Eq. (25) for time $t+2\tau$, namely,

$$r(t+2\tau)=r(t+\tau)+v(t+\tau)\tau+\frac{1}{2}\frac{f(t+\tau)}{m}\tau^2, \tag{27}$$

and subtract Eq. (25) from Eq. (27) to obtain

$$r(t+2\tau)=2r(t+\tau)-r(t)+[v(t+\tau)-v(t)]\tau + \frac{1}{2}\frac{f(t+\tau)-f(t)}{m}\tau^2. \tag{28}$$

If we substitute Eq. (26) in Eq. (28), we obtain

$$r(t+2\tau)=2r(t+\tau)-r(t)+\frac{f(t+\tau)}{m}\tau^2, \tag{29}$$

which is the position-Verlet algorithm in Eq. (22).

D. Predictor-corrector algorithm

Predictor-corrector algorithms consist of two-step processes in which the values of $r(t)$, for example, are first approximated by a predictor step and then adjusted by a corrector step. Before introducing one such method, let us write the equations of motion in the general form $dy/dt=F(y)$. One common implementation of a predictor-corrector method is a fourth-order algorithm that uses the explicit Adams-Bashforth four-step method given by[26]

$$y(t+\tau)=y(t)+\frac{\tau}{24}[55F(y(t))-59F(y(t-\tau)) + 37F(y(t-2\tau))-9F(y(t-3\tau))] \tag{30}$$

as the predictor step, and the implicit Adams-Moulton three-step method[26] given by

$$y(t+\tau)=y(t)+\frac{\tau}{24}[9F(y(t+\tau))+19F(y(t)) - 5F(y(t-\tau))+F(y(t-2\tau))] \tag{31}$$

as the corrector step. Both the predictor and the corrector steps have a local truncation error of $\mathcal{O}(\tau^5)$. The values of $y(t)$ for the initial three time steps, namely $y(\tau)$, $y(2\tau)$, and $y(3\tau)$, can be provided by three successive integrations of the equation of motion by other methods.

One advantage of this approach is that it is easy to apply to a general set of equations. However, it is usually not time reversible, does not preserve the phase-space volume, and yields large energy drifts unless very small time steps are used.

VI. DECOMPOSITION ALGORITHMS

Decomposition algorithms use an identity[7–10] to factorize the exponential operator $e^{(A+B)\tau}$. The simplest approximations are the lowest-order decompositions, namely

$$e^{(A+B)\tau}=e^{A\tau}e^{B\tau}+\mathcal{O}(\tau^2), \tag{32}$$

to first order, and

$$e^{(A+B)\tau}=e^{B\tau/2}e^{A\tau}e^{B\tau/2}+\mathcal{O}(\tau^3) \tag{33}$$

to second order. Equation (33) is equivalent to the Suzuki-Trotter decomposition used in quantum Monte Carlo simulations[27,28] in which A and B represent two noncommuting parts of the Hamiltonian.

Higher-order decompositions of the exponential operators have been derived.[7–10,12,29] The various decompositions express the exponential operator in terms of different numbers of separate operators, and have different truncation errors. For example, the fourth-order Suzuki-Trotter decomposition[10] factorizes the exponential operator $e^{(A+B)\tau}$ into a product of 15 terms.

A. Decomposition algorithms applied to molecular dynamics

We have seen in Sec. II that the evolution of the configuration of N particles, $y(t)$, can be written in the form of an evolution operator acting on $y(t)$. We now write the Liouville operator as a sum of two terms, namely

$$\hat{L}=\hat{L}_1+\hat{L}_2, \tag{34}$$

where the kinetic part corresponds to the free motion of the particles and is given by

$$\hat{L}_1=\sum_{i=1}^{N}\mathbf{v}_i\cdot\frac{\partial}{\partial\mathbf{r}_i}, \tag{35}$$

and the potential part is

$$\hat{L}_2=\sum_{i=1}^{N}\frac{\mathbf{f}_i}{m_i}\cdot\frac{\partial}{\partial\mathbf{v}_i}. \tag{36}$$

The equation of motion can be rewritten as

$$\frac{dy(t)}{dt}=(\hat{L}_1+\hat{L}_2)y(t), \tag{37}$$

for which the formal solution is

$$y(t+\tau)=e^{(\hat{L}_1\tau+\hat{L}_2\tau)}y(t). \tag{38}$$

The purpose of writing $\hat{L}=\hat{L}_1+\hat{L}_2$ is that the evolution operator can be decomposed using, for instance, Eq. (33) to yield

$$e^{(\hat{L}_1\tau+\hat{L}_2\tau)}=e^{\hat{L}_2\tau/2}e^{\hat{L}_1\tau}e^{\hat{L}_2\tau/2}+\mathcal{O}(\tau^3), \tag{39}$$

where the operator $e^{\hat{L}_1\tau}$ updates the positions of the particles and the operator $e^{\hat{L}_2\tau}$ updates the velocities, namely,

$$e^{\hat{L}_1\tau}y=\exp\left(\tau\sum_{j=1}^{N}\mathbf{v}_j\cdot\frac{\partial}{\partial\mathbf{r}_j}\right)\{\mathbf{r}_i,\mathbf{v}_i\}=\{\mathbf{r}_i+\mathbf{v}_i\tau,\mathbf{v}_i\}, \tag{40}$$

$$e^{\hat{L}_2\tau}y=\exp\left(\tau\sum_{j=1}^{N}\frac{\mathbf{f}_j}{m_j}\cdot\frac{\partial}{\partial\mathbf{v}_j}\right)\{\mathbf{r}_i,\mathbf{v}_i\}=\left\{\mathbf{r}_i,\mathbf{v}_i+\frac{\mathbf{f}_i}{m_i}\tau\right\}. \tag{41}$$

Note that the shift in the positions resulting from the operation described in Eq. (40) depends only on the velocities and the shift in the velocities in Eq. (41) involves only the forces and therefore only the positions.

Let us illustrate the explicit application of the second-order decomposition shown in Eq. (39) to perform the evolution of the equations of motion for molecular dynamics. First, we apply the right-most operator $e^{\hat{L}_2\tau/2}$ to $y(t)=\{\mathbf{r}_i(t),\mathbf{v}_i(t)\}$ to obtain

$$e^{\hat{L}_2\tau/2}\{\mathbf{r}_i(t),\mathbf{v}_i(t)\}=\left\{\mathbf{r}_i(t),\mathbf{v}_i(t)+\frac{\mathbf{f}_i(t)}{m_i}\frac{\tau}{2}\right\}. \tag{42}$$

We then apply the middle operator $e^{\hat{L}_1\tau}$ to Eq. (42) using Eq. (40), and find

$$\begin{aligned}
&e^{\hat{L}_1\tau}e^{\hat{L}_2\tau/2}\{\mathbf{r}_i(t),\mathbf{v}_i(t)\}\\
&\quad=e^{\hat{L}_1\tau}\left\{\mathbf{r}_i(t),\mathbf{v}_i(t)+\frac{\mathbf{f}_i(t)}{m_i}\frac{\tau}{2}\right\}\\
&\quad=\left\{\mathbf{r}_i(t)+\mathbf{v}_i\left(t+\frac{\tau}{2}\right)\tau,\mathbf{v}_i(t)+\frac{\mathbf{f}_i(t)}{m_i}\frac{\tau}{2}\right\}\\
&\quad=\left\{\mathbf{r}_i(t)+\mathbf{v}_i(t)\tau+\frac{\mathbf{f}_i(t)}{m_i}\frac{\tau^2}{2},\mathbf{v}_i(t)+\frac{\mathbf{f}_i(t)}{m_i}\frac{\tau}{2}\right\}.
\end{aligned} \tag{43}$$

Finally, the left-most operator $e^{\hat{L}_2\tau/2}$ is applied to Eq. (43), using Eq. (41), and yields

$$\begin{aligned}
&e^{\hat{L}_2\tau/2}e^{\hat{L}_1\tau}e^{\hat{L}_2\tau/2}\{\mathbf{r}_i(t),\mathbf{v}_i(t)\}\\
&\quad=e^{\hat{L}_2\tau/2}\left\{\mathbf{r}_i(t)+\mathbf{v}_i(t)\tau+\frac{\mathbf{f}_i(t)}{m_i}\frac{\tau^2}{2},\mathbf{v}_i(t)+\frac{\mathbf{f}_i(t)}{m_i}\frac{\tau}{2}\right\}\\
&\quad=\left\{\mathbf{r}_i(t)+\mathbf{v}_i(t)\tau+\frac{\mathbf{f}_i(t)}{m_i}\frac{\tau^2}{2},\mathbf{v}_i(t)\right.\\
&\qquad\left.+\frac{\mathbf{f}_i(t)}{m_i}\frac{\tau}{2}+\frac{\mathbf{f}_i(t+\tau)}{m_i}\frac{\tau}{2}\right\}.
\end{aligned} \tag{44}$$

Therefore, if we use the second-order decomposition method given in Eq. (33) to perform the evolution of the configuration, then $\mathbf{r}_i(t)$ and $\mathbf{v}_i(t)$ are updated as

$$\mathbf{r}_i(t+\tau)=\mathbf{r}_i(t)+\mathbf{v}_i(t)\tau+\frac{\mathbf{f}_i(t)}{m_i}\frac{\tau^2}{2}, \tag{45}$$

$$\mathbf{v}_i(t+\tau)=\mathbf{v}_i(t)+\frac{\mathbf{f}_i(t)}{m_i}\frac{\tau}{2}+\frac{\mathbf{f}_i(t+\tau)}{m_i}\frac{\tau}{2}, \tag{46}$$

which is equivalent to the velocity-Verlet algorithm discussed above. Note that the position-Verlet algorithm is equivalent to using Eq. (33) with A and B interchanged.[12,30] [This algorithm corresponds to using Eq. (39) with $\hat{L}_1$ and $\hat{L}_2$ interchanged on the right-hand side.]

Higher-order integration algorithms can be implemented using higher-order decompositions, such as the fourth-order Suzuki-Trotter decomposition.[10]

B. Decomposition algorithms applied to spin dynamics

A similar decomposition procedure can be applied to spin dynamics. We illustrate this procedure using the spin Hamiltonian in Eq. (9), which can be reexpressed with the help of Eq. (11) as

$$\mathcal{H}=\sum_i \mathbf{S}_i\cdot\mathbf{H}_{\mathrm{eff},i}. \tag{47}$$

The simple cubic lattice can be divided into two interpenetrating sublattices $\mathcal{A}$ and $\mathcal{B}$. Hence we can decompose the Hamiltonian into summations of spins in sublattice $\mathcal{A}$ and in sublattice $\mathcal{B}$:

$$\mathcal{H}=\sum_{i\in\mathcal{A}}\mathbf{S}_i\cdot\mathbf{H}_{\mathrm{eff},\mathcal{A}_i}+\sum_{i\in\mathcal{B}}\mathbf{S}_i\cdot\mathbf{H}_{\mathrm{eff},\mathcal{B}_i}, \tag{48}$$

where $\mathbf{H}_{\mathrm{eff},\mathcal{A}_i}$ and $\mathbf{H}_{\mathrm{eff},\mathcal{B}_i}$ are the effective fields acting on the spins $\mathbf{S}_i$ in sublattices $\mathcal{A}$ and $\mathcal{B}$, respectively. Following the derivations in Sec. III the equations of motion can be written as

$$\frac{d\mathbf{S}_i}{dt}=-\mathbf{S}_i\times\mathbf{H}_{\mathrm{eff},\mathcal{A}_i}-\mathbf{S}_i\times\mathbf{H}_{\mathrm{eff},\mathcal{B}_i}, \tag{49}$$

and reduced to the more compact form

$$\frac{dy(t)}{dt}=(\hat{R}_{\mathcal{A}}+\hat{R}_{\mathcal{B}})y(t), \tag{50}$$

where $\hat{R}_{\mathcal{A}}$ and $\hat{R}_{\mathcal{B}}$ are defined in a similar way as the operator $\hat{R}$ in Eqs. (14)–(17), but with nonzero effective fields for spins in sublattices $\mathcal{A}$ and $\mathcal{B}$, respectively, and $\hat{R}_{\mathcal{A}}+\hat{R}_{\mathcal{B}}=\hat{R}$. The formal solution to the equations of motion is

$$y(t+\tau)=e^{(\hat{R}_{\mathcal{A}}+\hat{R}_{\mathcal{B}})\tau}y(t). \tag{51}$$

We decompose the evolution operator using Eq. (33) and obtain

$$e^{(\hat{R}_{\mathcal{A}}+\hat{R}_{\mathcal{B}})\tau}=e^{\hat{R}_{\mathcal{B}}\tau/2}e^{\hat{R}_{\mathcal{A}}\tau}e^{\hat{R}_{\mathcal{B}}\tau/2}+\mathcal{O}(\tau^3), \tag{52}$$

where $e^{\hat{R}_{\mathcal{A}}\tau}$ rotates the spins $\mathbf{S}_i$ in sublattice $\mathcal{A}$ by an angle $|\mathbf{H}_{\mathrm{eff},\mathcal{A}_i}|\tau$ around $\mathbf{H}_{\mathrm{eff},\mathcal{A}_i}$ while keeping spins in sublattice $\mathcal{B}$ fixed, and $e^{\hat{R}_{\mathcal{B}}\tau}$ rotates the spins in sublattice $\mathcal{B}$ by an angle $|\mathbf{H}_{\mathrm{eff},\mathcal{B}_i}|\tau$ around $\mathbf{H}_{\mathrm{eff},\mathcal{B}_i}$ while keeping the spins in sublattice $\mathcal{A}$ fixed. (Appendix B explains why the evolution operator rotates the spins around their effective fields.) Because these operators rotate a spin around its effective field, which is fixed during this rotation, the scalar products of spins are preserved in each of these operations; therefore the spin length and the energy are conserved exactly (within machine precision). The effective fields acting on the spins of a given sublattice are determined only by the spins on the other sublattice; therefore, the rotations of all the spins on one sublattice are independent of each other and can be done in parallel. Decomposition algorithms are easy to implement because the separate operators $e^{\hat{R}_{\mathcal{A}}\tau}$ and $e^{\hat{R}_{\mathcal{B}}\tau}$ have a simple explicit form.[13]

As for molecular dynamics, higher-order integration algorithms for spin dynamics can be implemented using higher-order decompositions of the exponential operator.

C. Properties of the decomposition algorithms

The above decomposition algorithms preserve the phase space volume element in molecular and spin dynamics simulations. For molecular dynamics the operator $e^{\hat{L}_1\tau}$ ($e^{\hat{L}_2\tau}$) acting on y shifts $\mathbf{r}_i$ ($\mathbf{v}_i$), and the shift depends only on the $\mathbf{v}_i$ ($\mathbf{r}_i$), as shown in Eqs. (40) and (41). For spin dynamics the operator $e^{\hat{R}_{\mathcal{A}}\tau}$ ($e^{\hat{R}_{\mathcal{B}}\tau}$) acting on y rotates the spins in sublattice $\mathcal{A}$ ($\mathcal{B}$) with the spins in sublattice $\mathcal{B}$ ($\mathcal{A}$) fixed. Therefore, in both cases the Jacobian of the transformation from $y(t)$ to $y(t+\tau)$ is equal to one, and hence the phase-space volume is preserved.

In our examples, the decompositions of the exponential operator $e^{(A+B)\tau}$ are of even order and the operators $e^{A\tau}$ and

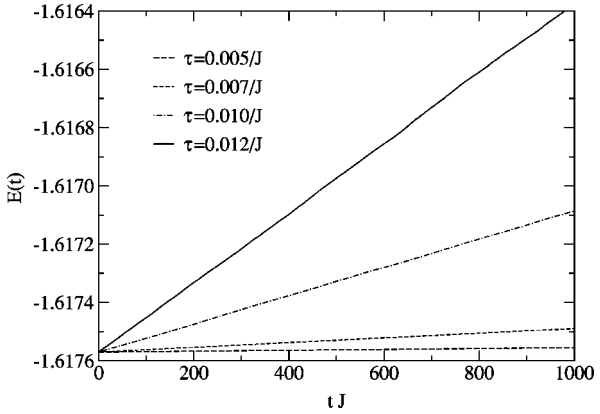

Fig. 1. Energy per site versus time for the Heisenberg model described in the text obtained with the fourth-order predictor-corrector method in Eqs. (30) and (31). The curves are for different integration time steps τ and a single initial configuration.

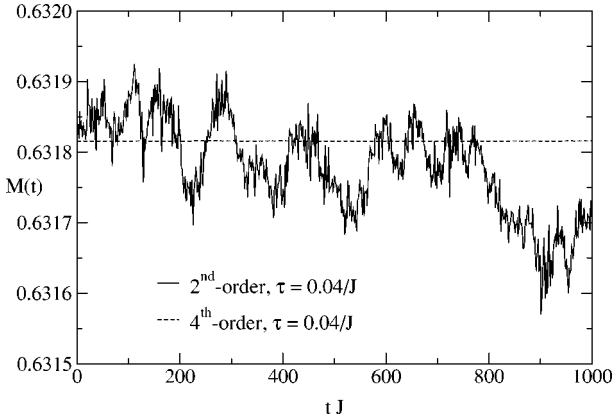

Fig. 2. Comparison of fluctuations in the uniform magnetization per site for the second- and fourth-order Suzuki-Trotter decomposition with $\tau=0.04/J$ for a single initial configuration. Data are for the Heisenberg ferromagnet described in the text.

$e^{B\tau}$ enter symmetrically in the decomposition. Therefore the product of the operators $e^{B\tau/2}e^{A\tau}e^{B\tau/2}$ is time symmetric. By defining

$$\hat{U}(\tau)\equiv e^{B\tau/2}e^{A\tau}e^{B\tau/2}, \tag{53}$$

we obtain

$$\hat{U}(\tau)\hat{U}(-\tau)=e^{B\tau/2}e^{A\tau}e^{B\tau/2}e^{-B\tau/2}e^{-A\tau}e^{-B\tau/2}=1. \tag{54}$$

Similarly, $\hat{U}(-\tau)\hat{U}(\tau)=1$. Hence each time step in the evolution using Eq. (33) is reversible, leading to a time reversible trajectory. This proof can be easily extended to higher-order decompositions.

Although the decomposition algorithm does not conserve the total energy of a general system, the long-term energy deviation as a function of time is characterized by a random walk, that is, it does not display a systematic drift in any direction. This behavior is due to the time reversibility property shown in Eq. (54) and applies to other conserved quantities as well, as we will illustrate in the following. In addition, the higher-order integration methods are accurate for larger time steps, allowing simulations to reach longer times without generating large truncation errors.

Higher-order decomposition algorithms require more operations, and hence more cpu time per integration step. However, they are accurate for larger time steps, and they are more efficient if the decrease in the number of time steps compensates for the slower integration step. Higher-order decompositions also are more advantageous if the system studied requires that the conservation laws be obeyed more strictly.

D. Algorithm performance

The performance of some of the algorithms will be illustrated by simulations of a Heisenberg ferromagnet on a $10\times10\times10$ simple cubic lattice at temperature $T=0.8\,T_c$, where T_c is the critical temperature of the model. The equations of motion conserve both the total energy per site $E(t)$ and the uniform magnetization per site $M(t)$ of the system. The fourth-order predictor-corrector method in Eqs. (30) and (31) conserves the uniform magnetization exactly; however, the total energy drifts systematically and considerably, even for relatively small time steps, as shown in Fig. 1.

In contrast, the decomposition algorithms conserve both the energy and the spin length exactly, because the scalar product of nearest-neighbor spins is preserved during the rotation of a spin around its effective field. The uniform magnetization is not exactly conserved by the decomposition algorithms; however, there is no long time drift in the magnetization, as illustrated in Fig. 2 for the second- and fourth-order Suzuki-Trotter decomposition[10] with $\tau=0.04/J$. Figure 2 also shows that for the same time step, higher-order methods yield smaller magnetization fluctuations. The fluctuations of the magnetization per site $M(t)$ for the second- and fourth-order algorithm are $\sim4\times10^{-4}$ and $\sim1.5\times10^{-6}$, respectively (see Fig. 2).

Figure 3 shows the fluctuations in the magnetization per site using a fourth-order Suzuki-Trotter decomposition with different time steps. In Fig. 3, the magnetization fluctuations for $\tau=0.1/J$ and $0.2/J$ are $\sim1.2\times10^{-5}$ and $\sim1\times10^{-4}$, respectively, for a maximum time of $1000/J$.

Each integration step of the predictor-corrector method in Eqs. (30) and (31) is approximately 2.5 times faster than each step using the fourth-order Suzuki-Trotter decomposition. However, the latter generates results that are accurate for much larger time steps, and thus constitutes a much faster

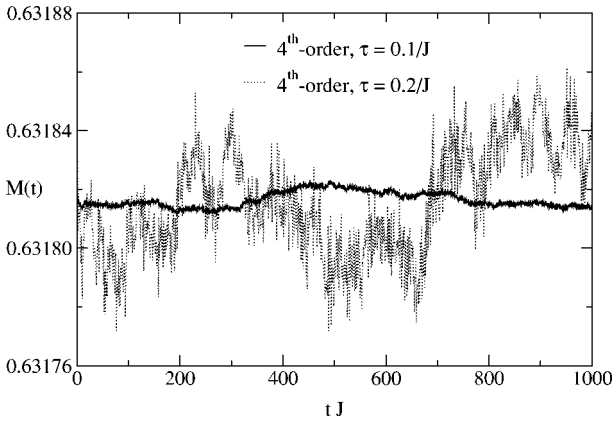

Fig. 3. Comparison of fluctuations in the uniform magnetization per site for a fourth-order Suzuki-Trotter decomposition with different time steps τ for a single initial configuration. For the Heisenberg ferromagnet described in the text.

algorithm. For example, the equations of motion of a Heisenberg ferromagnet on a $10\times10\times10$ simple cubic lattice can be integrated using the fourth-order predictor-corrector method in Eqs. (30) and (31) with $\tau=0.01/J$. The cpu time required to reach a time of $t=500/J$ (which corresponds to 50 000 integration steps) is $\approx$18.7 s on a 1.3 GHz Pentium 4 processor. The fourth-order Suzuki-Trotter decomposition algorithm allows us to use $\tau=0.20/J$, and the cpu time to reach the same time (that is, 2500 integration steps) is approximately 2.2 s, which corresponds to a speed up of about a factor of 8. Even higher-order methods provide even better magnetization conservation,[31,32] but may not be very competitive in terms of computational efficiency, because they require a much larger number of spin rotations per time step, which significantly increases the cpu time usage of the algorithm.

E. Further developments

Decompositions of exponential operators into terms that involve higher-order derivatives of the variables in the equations of motion, such as force gradients for molecular dynamics, have been implemented and shown to be more advantageous for some applications.[33–35]

For systems with different time scales, such as magnetic materials with both strong exchange (short time scale) and weak dipolar (long time scale) interactions, decomposition methods can be used to integrate the slow varying components of the system with a larger time step than the rapidly varying components.[36,37] As an example, assume that the Liouville operator can be separated into a slow and a rapidly varying part denoted as L_s and L_f, respectively. The second-order decomposition given by Eq. (33) can be further decomposed into

$$e^{(L_f+L_s)\tau}=e^{L_s\tau/2}[e^{L_f\delta}]^n e^{L_s\tau/2}+\mathcal{O}(\tau^3), \tag{55}$$

where $\tau/2$ is the time step used for the slow dynamics, n is an integer, and $\delta=\tau/n$ is a smaller time step used to evolve the fast dynamics of the system.

Depending on the dynamics and types of interactions in the system, it may be necessary to decompose the exponential operator into more than two individual operators. For example, spin dynamics simulations of a spin system on a triangular lattice with nearest-neighbor interactions require a three-sublattice decomposition, and the second-order decomposition can be written as

$$e^{(A+B+C)\tau}=e^{A\tau/2}e^{B\tau/2}e^{C\tau}e^{B\tau/2}e^{A\tau/2}+\mathcal{O}(\tau^3), \tag{56}$$

where each of the three separate operators $e^{A\tau}$, $e^{B\tau}$, and $e^{C\tau}$ rotates the spins on one sublattice with the spins on the other two sublattices fixed. Spin dynamics simulations of an antiferromagnetic XY model on the triangular lattice have been done using a second-order decomposition algorithm[38] described in Eq. (56). The dynamic behavior of the system was studied for a range of temperatures, including the Kosterlitz-Thouless transition and the Ising transition, where long-range order appears in the staggered chirality.[38] There are several other applications in the literature that require decompositions involving multiple operators.[39]

VII. SPIN DYNAMICS RESULTS

Figure 4 shows the dynamic structure factor[6] $S(q,\omega)$, for momentum transfer $\mathbf{q}=(q,0,0)$ and frequency ω, for the Heisenberg ferromagnet described in Eq. (9) on a $20\times20\times20$ simple cubic lattice at $T=0.4\ T_c$ and various values of q. The dynamic structure factor can be used to detect and characterize collective excitations, such as spin waves in a magnetic system, and can be measured in neutron scattering experiments. The integration of the equations of motion were done up to $t_{\max}=1000/J$ using a fourth-order Suzuki-Trotter decomposition[10] with a time step of $\tau=0.2/J$.

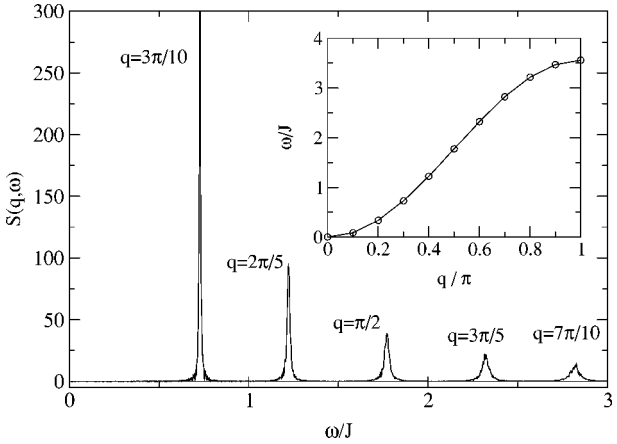

Fig. 4. Dynamic structure factor $S(q,\omega)$ and dispersion curve (inset) for the Heisenberg ferromagnet on the simple cubic lattice with $L=20$ at $T=0.4\ T_c$. The momentum transfer is in the [100] direction, that is, $\mathbf{q}=(q,0,0)$, and the Brillouin zone boundary is at $q=\pi$.

The inset of Fig. 4 shows the dispersion curve[40] of the collective excitations, that is, the frequencies of the spin wave peaks as a function of q. Spin dynamics of $RbMnF_3$ have been performed on simple cubic lattices with linear sizes up to $L=72$, which corresponds to solving a system of $72^3=373\,248$ equations.[16] A direct comparison of $S(\mathbf{q},\omega)$ obtained from spin dynamics simulations and neutron scattering data[22] yields good quantitative agreement, with no adjustable parameters.[15] An illustration of this comparison at $T=0.894\ T_c$ for $\mathbf{q}$ in the [111] direction is shown in Fig. 5. The experimental energy resolution width was 0.25 meV, which is shown as a horizontal line segment in Fig. 5. The

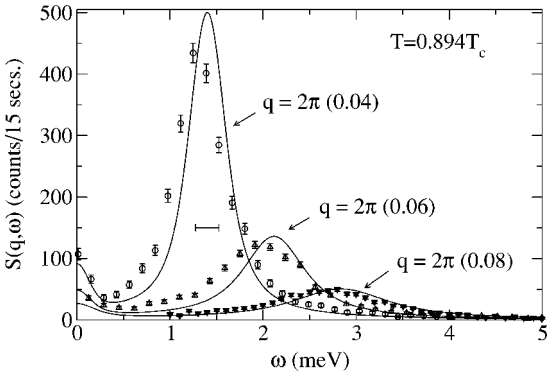

Fig. 5. Comparison of dynamic structure factor as a function of frequency from simulation and experiment, for $T=0.894\ T_c$ and $\mathbf{q}=(q,q,q)$. The symbols represent neutron scattering data [the circles, triangles, and inverted triangles correspond to $q=2\pi(0.04)$, $2\pi(0.06)$, and $2\pi(0.08)$, respectively]; the solid lines are simulation results for $L=60$. No adjustable parameters were used for the comparison. The horizontal line segment indicates the experimental energy resolution.

values of $S(q,\omega)$ from the simulations were convoluted with the experimental resolution function and the T- and ω-dependent population factor was removed from the neutron scattering data. The normalization of the intensities of $S(q,\omega)$ between simulation and experiment was done at one T and q; the same factor was then used to normalize the curves for all values of q.

Suggested problem: Apply a second-order Suzuki-Trotter decomposition algorithm to integrate the equations of motion of an isotropic Heisenberg ferromagnet on a simple cubic lattice with $L=10$. Use a few initial spin configurations at $T=0.8\ T_c$. For each case determine the energy and magnetization as a function of time. Observe how well these quantities are conserved and how the fluctuations vary with increasing time steps. Spin waves can be observed by plotting the spins as a function of time.

VIII. SUMMARY

Molecular dynamics and spin dynamics simulations require good algorithms for the integration of the equations of motion. Desirable properties of integration algorithms include accuracy for long time steps, time reversibility, good conservation of energy, and being symplectic (conserving phase-space volume).

The standard integration algorithms used in applied mathematics are neither time reversible nor symplectic, and yield large long-term energy drift unless very small time steps are used. In contrast, algorithms based on the decomposition of exponential operators are time reversible, symplectic, and have bounded energy fluctuations. In some cases, such as for the Heisenberg ferromagnet described in Eq. (9), the energy can be conserved exactly (within machine precision). Decomposition algorithms also are accurate for larger time steps and allow integration to much longer times. These methods are broadly applicable and may be straightforwardly applied to more complicated systems, although the decompositions may involve more than two operators, leading to an increase in complexity.

ACKNOWLEDGMENTS

This work was supported in part by NSF Grant No. DMR-0341874. We are indebted to Michael Krech and Kwangsik Nho for very helpful discussions, and to Larry Engelhardt and Rodrigo Freire for their critical reading of this manuscript.

APPENDIX A: PROOF OF FORMAL SOLUTION OF THE EQUATIONS OF MOTION

Some basic properties of the evolution operator will be presented before the proof of the formal solution is derived.[41] A generic time evolution operator $U(t)$, where the argument t represents the time, must be a continuous operator of the parameter t and satisfy the following conditions:

$$U(t=0)=I, \tag{A1}$$

$$U(t_1+t_2)=U(t_1)U(t_2)=U(t_2)U(t_1), \tag{A2}$$

$$U(-t)=U^{-1}(t). \tag{A3}$$

We shall now derive an expression for the time derivative of $U(t)$,

$$\frac{dU(t)}{dt}=\lim_{\delta t\to 0}\frac{U(t+\delta t)-U(t)}{\delta t}. \tag{A4}$$

If we use Eq. (A2), we can write

$$U(t+\delta t)=U(t)U(\delta t)=U(\delta t)U(t). \tag{A5}$$

By substituting Eq. (A5) into Eq. (A4) and using Eq. (A1), we have

$$\frac{dU(t)}{dt}=\left[\lim_{\delta t\to 0}\frac{U(\delta t)-U(0)}{\delta t}\right]U(t)=\left[\frac{dU(t)}{dt}\right]_{t=0}U(t). \tag{A6}$$

Let $G\equiv[dU(t)/dt]_{t=0}$. Then by taking successive time derivatives of Eq. (A6) and repeatedly using Eq. (A6), it is easy to show that

$$\frac{d^nU(t)}{dt^n}=G^nU(t). \tag{A7}$$

Equation (A7) is very important because it allows us to write $U(t)$ in terms of G by expanding $U(t)$ in a Taylor series about $t=0$:

$$\begin{aligned}U(t)&=1+\left[\frac{dU(t)}{dt}\right]_{t=0}t+\left[\frac{d^2U(t)}{dt^2}\right]_{t=0}\frac{t^2}{2!}+\cdots\\&=1+Gt+\frac{(Gt)^2}{2!}+\cdots.\end{aligned} \tag{A8}$$

We conclude that

$$U(t)=\exp(Gt). \tag{A9}$$

Now we are ready to derive the formal solution to the equations of motion that appear in molecular and spin dynamics simulations. Given the differential equation

$$\frac{dy(t)}{dt}=Gy(t), \tag{A10}$$

let $U(\tau)=\exp(G\tau)$. To show that

$$y(t_0+\tau)=U(\tau)y(t_0)=\exp(G\tau)y(t_0) \tag{A11}$$

is a solution to Eq. (A10), it is sufficient to verify that it satisfies Eq. (A10). We differentiate Eq. (A11) with respect to the time $t=t_0+\tau$ and set $\tau=0$. Because t_0 is fixed, we have

$$\left.\frac{dy(t)}{dt}\right|_{t=t_0}=\left.\frac{dU(\tau)}{d\tau}\right|_{\tau=0}y(t_0)=Gy(t_0). \tag{A12}$$

Therefore, $dy(t_0)/dt_0=Gy(t_0)$ for arbitrary t_0 or $dy(t)/dt=Gy(t)$ in general. Hence Eq. (A11) is a solution to Eq. (A10).

APPENDIX B: THE EVOLUTION OPERATOR IN SPIN DYNAMICS

We explain here why the evolution operator in spin dynamics rotates the spins around their effective fields. For simplicity, consider the equation of motion for one spin given in Eq. (12). For an infinitesimal time displacement dt Eq. (12) yields (to simplify the notation we drop the subscript i)

$$\mathbf{S}(t+dt)=\mathbf{S}(t)+(\mathbf{H}_{\text{eff}}\times\mathbf{S}(t))dt. \tag{B1}$$

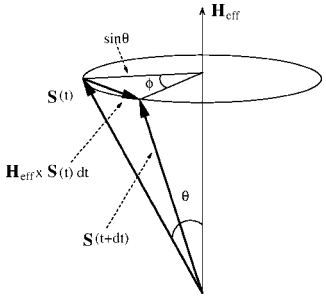

Fig. 6. Evolution of a spin by an infinitesimal time step dt.

We denote the angle between $\mathbf{S}(t)$ and $\mathbf{H}_{\text{eff}}$ as θ as shown in Fig. 6. Note that $\mathbf{S}(t+dt)$ in Eq. (B1) consists of a rotation of $\mathbf{S}(t)$ around $\mathbf{H}_{\text{eff}}$ by an angle ϕ. Because dt is infinitesimal, we can write

$$\phi = \frac{|\mathbf{H}_{\text{eff}} \times \mathbf{S}(t)|dt}{\sin\theta} = \frac{|\mathbf{H}_{\text{eff}}||\mathbf{S}(t)|\sin\theta\, dt}{\sin\theta} = |\mathbf{H}_{\text{eff}}|dt, \tag{B2}$$

where we have used that $|\mathbf{S}(t)| = 1$.

The equation of motion in the form given in Eq. (14) yields

$$\mathbf{S}(t+dt) = \mathbf{S}(t) + R\mathbf{S}(t)dt = (1+Rdt)\mathbf{S}(t). \tag{B3}$$

After another infinitesimal time step, we have

$$\mathbf{S}(t+2dt) = (1+Rdt)\mathbf{S}(t+dt) = (1+Rdt)^2\mathbf{S}(t). \tag{B4}$$

By induction we obtain

$$\mathbf{S}(t+ndt) = (1+Rdt)^n\mathbf{S}(t), \tag{B5}$$

where n is an integer number of infinitesimal time steps. For a finite time step, $\tau = ndt$, we have

$$\mathbf{S}(t+\tau) = \lim_{n\to\infty}\left(1+R\frac{\tau}{n}\right)^n \mathbf{S}(t) = e^{R\tau}\mathbf{S}(t). \tag{B6}$$

Each of the n infinitesimal updates of $\mathbf{S}(t)$ is a rotation of this spin around its effective field $\mathbf{H}_{\text{eff}}$ by an angle $|\mathbf{H}_{\text{eff}}|dt$. Because the finite time step τ is composed of n infinitesimal rotations, the finite time evolution operator $e^{R\tau}$ consists of a rotation of $\mathbf{S}(t)$ around $\mathbf{H}_{\text{eff}}$ by the angle $|\mathbf{H}_{\text{eff}}|\tau$.

This derivation of the effect of the application of the evolution operator on one spin can be extended to all spins of the lattice by using the notation $y(t)$ defined in Eq. (16). The challenge is to find a practical way to perform the rotations of all spins. This challenge is nontrivial because the rotations are interconnected, that is, rotating one spin generates a new effective field for its nearest neighbors. A practical solution is to use decompositions of the evolution operators as described in Sec. VI B.

[1]See, for example, *Monte Carlo Methods in Statistical Physics*, edited by K. Binder (Springer-Verlag, New York, 1986); *Applications of the Monte Carlo Method in Statistical Physics*, edited by K. Binder (Springer-Verlag, New York, 1987); *The Monte Carlo Method in Condensed Matter Physics*, edited by K. Binder (Springer-Verlag, New York, 1996).

[2]See, for example, H. Gould and J. Tobochnik, *An Introduction to Computer Simulation Methods* (Addison-Wesley, Reading, MA, 1996), and D. P. Landau and K. Binder, *A Guide to Monte Carlo Simulations in Statistical Physics* (Cambridge U.P., Cambridge, 2000).

[3]D. P. Landau, S.-H. Tsai, and M. Exler, "A new approach to Monte Carlo simulations in statistical physics: Wang-Landau sampling," Am. J. Phys. **72**, 1294–1302 (2004).

[4]D. P. Landau and R. Alben, "Monte Carlo calculations as an aid in teaching statistical mechanics," Am. J. Phys. **41**, 394–400 (1973).

[5]See, for example, M. P. Allen and D. J. Tildesley, *Computer Simulation of Liquids* (Oxford U.P., Oxford, 1987); D. Frenkel and B. Smit, *Understanding Molecular Simulation*, 2nd ed. (Academic, New York, 2002).

[6]D. P. Landau and M. Krech, "Spin dynamics simulations of classical ferro- and antiferromagnetic model systems: Comparison with theory and experiment," J. Phys.: Condens. Matter **11**, R179–R213 (1999).

[7]H. Yoshida, "Construction of higher order symplectic integrators," Phys. Lett. A **150**, 262–268 (1990).

[8]E. Forest and R. D. Ruth, "Fourth-order symplectic integration," Physica D **43**, 105–117 (1990).

[9]M. Suzuki, "General theory of higher-order decomposition of exponential operators and symplectic integrators," Phys. Lett. A **165**, 387–395 (1992).

[10]M. Suzuki and K. Umeno, "Higher-order decomposition theory of exponential operators and its applications to QMC and nonlinear dynamics," in *Computer Simulation Studies in Condensed Matter Physics VI*, edited by D. P. Landau, K. K. Mon, and H.-B. Schüttler (Springer-Verlag, Berlin, 1993), pp. 74–86.

[11]M. E. Tuckerman and G. J. Martyna, "Understanding modern molecular dynamics: Techniques and applications," J. Phys. Chem. B **104**, 159–178 (2000).

[12]I. P. Omelyan, I. M. Mryglod, and R. Folk, "Symplectic analytically integrable decomposition algorithms: Classification, derivation, and application to molecular dynamics, quantum and celestial mechanics simulations," Comput. Phys. Commun. **151**, 272–314 (2003).

[13]M. Krech, A. Bunker, and D. P. Landau, "Fast spin dynamics algorithms for classical spin systems," Comput. Phys. Commun. **111**, 1–13 (1998).

[14]J. Frank, W. Huang, and B. Leimkuhler, "Geometric integrators for classical spin systems," J. Comput. Phys. **133**, 160–172 (1997).

[15]S.-H. Tsai, A. Bunker, and D. P. Landau, "Spin-dynamics simulations of the magnetic dynamics of $RbMnF_3$ and direct comparison with experiment," Phys. Rev. B **61**, 333–342 (2000).

[16]S.-H. Tsai and D. P. Landau, "Critical dynamics of the simple-cubic Heisenberg antiferromagnet $RbMnF_3$: Extrapolation to $q=0$," Phys. Rev. B **67**, 104411-1–6 (2003).

[17]See, for example, C. Kittel, *Introduction to Solid State Physics*, 6th ed. (J. Wiley, New York, 1986), pp. 430–448.

[18]See, for example, R. W. Gerling, "Computer simulations of spin solitons in magnetic chains," Comput. Phys. Rep. **7**, 73–146 (1988).

[19]See, for example, P. C. Hohenberg and B. I. Halperin, "Theory of dynamic critical phenomena," Rev. Mod. Phys. **49**, 435–479 (1977).

[20]See, for example, H. Goldstein, C. P. Poole, and J. L. Safko, *Classical Mechanics*, 3rd ed. (Addison-Wesley, Reading, MA, 2002).

[21]C. G. Windsor and R. W. H. Stevenson, "Spin waves in $RbMnF_3$," Proc. Phys. Soc. **87**, 501–504 (1966).

[22]See, for example, R. Coldea, R. A. Cowley, T. G. Perring, D. F. McMorrow, and B. Roessli, "Critical behavior of the three-dimensional Heisenberg antiferromagnet $RbMnF_3$," Phys. Rev. B **57**, 5281–5290 (1998).

[23]D. S. Ritchie and M. E. Fisher, "Theory of critical-point scattering and correlations. II. Heisenberg models," Phys. Rev. B **5**, 2668–2692 (1972).

[24]See, for example, A. H. Morrish, *The Physical Principles of Magnetism* (J. Wiley, New York, 1966), pp. 106–111.

[25]See, for example, W. H. Press, S. A. Teukolsky, W. T. Vetterling, and B. P. Flannery, *Numerical Recipes*, 2nd ed. (Cambridge U.P., Cambridge, 1992).

[26]See, for example, R. L. Burden and J. D. Faires, *Numerical Analysis*, 4th ed. (PWS-KENT, Boston, 1989), p. 265.

[27]M. Suzuki, "Relationship between d-dimensional quantal spin systems and $(d+1)$-dimensional Ising systems," Prog. Theor. Phys. **56**, 1454–1469 (1976).

[28]M. Suzuki, S. Miyashita, and A. Kuroda, "Monte Carlo simulation of quantum spin systems. I," Prog. Theor. Phys. **58**, 1377–1387 (1977).

[29]I. P. Omelyan, I. M. Mryglod, and R. Folk, "Optimized Forest-Ruth- and Suzuki-like algorithms for integration of motion in many-body systems," Comput. Phys. Commun. **146**, 188–202 (2002).

[30]I. P. Omelyan, I. M. Mryglod, and R. Folk, "Optimized Verlet-like algorithms for molecular dynamics simulations," Phys. Rev. E **65**, 056706-1–5 (2002).

[31]D. P. Landau, S.-H. Tsai, M. Krech, and A. Bunker, "Improved spin dynamics simulations of magnetic excitations," Int. J. Mod. Phys. C **10**, 1541–1551 (1999).

[32]S.-H. Tsai, M. Krech, and D. P. Landau, Braz. J. Phys. **34**, 384–391 (2004).
[33]M. Suzuki, ''Hybrid exponential product formulas for unbounded operators with possible applications to Monte Carlo simulations,'' Phys. Lett. A **201**, 425–428 (1995).
[34]S. A. Chin, ''Symplectic integrators from composite operator factorizations,'' Phys. Lett. A **226**, 344–348 (1997).
[35]I. P. Omelyan, I. M. Mryglod, and R. Folk, ''Construction of high-order force-gradient algorithms for integration of motion in classical and quantum systems,'' Phys. Rev. E **66**, 026701-1–21 (2002).
[36]M. Tuckerman, B. J. Berne, and G. J. Martyna, ''Reversible multiple time scale molecular dynamics,'' J. Chem. Phys. **97**, 1990–2001 (1992).
[37]S. J. Stuart, R. Zhou, and B. J. Berne, ''Molecular dynamics with multiple time scales: The selection of efficient reference system propagators,'' J. Chem. Phys. **105**, 1426–1436 (1996).
[38]K. Nho and D. P. Landau, ''Spin-dynamics simulations of the triangular antiferromagnetic XY model,'' Phys. Rev. B **66**, 174403-1–7 (2002).
[39]For example, see I. P. Omelyan, I. M. Mryglod, and R. Folk, ''Algorithm for molecular dynamics simulations of spin liquids,'' Phys. Rev. Lett. **86**, 898–901 (2001).
[40]See, for example, N. W. Ashcroft and N. D. Mermin, *Solid State Physics* (Saunders College, New York, 1976), p. 709.
[41]A. Bohm, *Quantum Mechanics: Foundations and Applications* (Springer-Verlag, New York, 1994).

Ayrton and Perry's Variable Standard of Self-Induction. This is a classic piece of electrical measurement apparatus made by Leeds & Northrup of Philadelphia. The two coils are connected together in a series. The outer one is fixed, while the inner one can be rotated to vary the coupling between the coils. The wood forms are seasoned and laminated to provide maximum geometrical stability. The range was from 3.5 to 42 millihenrys. The apparatus, at Denison University, is listed in the first (1903) L&N catalogue at $125. Note the correct spelling of Ayrton's name, which was misspelled in the note on Ayrton and Perry's Sechometer, *Am. J. Phys.* **72**, 1403 (2004). (Photograph and Notes by Thomas B. Greenslade, Jr., Kenyon College)